August 14, 2008

Double-Lepton Polarization Asymmetries and Polarized Forward Backward Asymmetries in The Rare $b \to s\ell^+\ell^-$ Decays in a Single Universal Extra Dimension Scenario

V. Bashiry[1]*, M. Bayar[2]†, K. Azizi[2]‡,

[1] Engineering Faculty, Cyprus International University,

Via Mersin 10, Turkey

[2] Physics Department, Middle East Technical University,

06531 Ankara, Turkey

Abstract

We study the double-lepton polarization asymmetries and single and double-lepton polarization forward backward asymmetries of the rare $b \to s\ell^+\ell^-$ mode within the Standard Model and in the Appelquist-Cheng-Dobrescu model, which is a new physics scenario with a single universal extra dimension. In particular, we examine the sensitivity of the observables to the radius R of the compactified extra-dimension, which is the new parameter in this new physics model.

PACS numbers: 12.60.-i, 13.25.Hw

*e-mail: bashiry@ciu.edu.tr

†e-mail: mbayar@newton.physics.metu.edu.tr

‡e-mail: e146342@metu.edu.tr

1 Introduction

The standard model (SM) has been successful theory in reproducing almost all experimental data about the interaction of gauge bosons and fermions. However, the SM is not regarded as a full theory, since it can not address some issues such as stability of the scalar sector under radiative corrections, gauge and fermion mass hierarchy, matter-antimatter asymmetry, number of generations and so on. For these reasons, It is well known that the SM need to be extended in a way where the SM can be considered as a low energy manifestation of some fundamental theory or alternative theories must used instead of the SM.

Extra dimension (ED) model with a flat metric proposed by Arkani et. al. [1] or with small compactification radius is one of the candidates trying to shed light on some of those issues as well as to provide a unified framework for gravity and the other interactions together with a connection with the string theory [1]. It can be categorized in terms of the mechanism of new physics (NP) where the SM fields are constrained to move in the usual three spatial dimensions (D_3 bran) or can propagate in the extra dimensions (the bulk). The last one can be categorized as non–universal extra dimension (NUED) and universal extra dimension (UED). In the non universal model, the gauge bosons propagate into the bulk, but the fermions are confined to D_3 bran. In contrast, the UED, which is the most democratic, allows fields to propagate into the bulk. The UED can be considered as a generalization of the usual SM to a D_{3+N} bran where N is the number of the extra dimensions[2]. The first proposal for using large (TeV) extra dimensions in the SM proposed by I. Antoniadis [3] who worked out the main consequences. The model introduced by Appelquist, Cheng and Dobrescu (ACD) [4] is the most simple example of the UED where just single universal extra dimension is considered. This model has only one free parameter in addition to the SM parameters and that is the compactification scale R. The ACD model is a particular model within the same general idea proposed in [3]. Mass of the Kaluza-Klein(KK) particles are inversely proportional to R, then, above some compactification scale $1/R$ the models are higher dimensional theories whose equivalent description in four dimensions includes the ordinary SM fields together with towers of their Kaluza-Klein (KK) excitations and other fields having no standard model partners[5].

Two types of study can be conducted to explore extra dimensions. In the direct search, the center of mass energy of colling particles must be increased to produce Kaluza-Klein(KK) excitation states, where KK excitation states are supposed to produce in pair by KK number conservation. On the other hand, we can investigate UED effects, indirectly. The indirect search at tree-level, where KK excitations can contribute as a mediator, is suppressed by KK number conservation. On the contrary, the same states can contribute to the quantum loop level where the KK number conservation is broken. As a result, flavor changing neutral current(FCNC) transition induced by quantum loop level can be considered as a good tool for studying KK effects. The collider signatures and phenomenology of UED have been studied by Ref. [2] and [6, 7], respectively. These studies have provided a theoretical framework to investigate some inclusive and exclusive decays with the ACD.

FCNC and CP-violating are indeed the most sensitive probes of NP contributions to penguin operators. Rare decays, induced by FCNC of $b \to s(d)$ transitions are at the forefront of our quest to understand flavor and the origins of CP violation asymmetry (CPV), offering one of the best probes for NP beyond the SM, in particular to probe

extra dimension. In this regard, the semileptonic and pureleptonic B decays have been studied with UED scenario[6]–[11]. They have obtained that the inclusive and exclusive semileptonic and pureleptonic decays are sensitive to the new parameter coming out of the one universal extra dimensions i.e., compactification scale $1/R$.

New physics effects manifest themselves in rare decays in different ways: NP can contribute through the new Wilson coefficients or the new operator structure in the effective Hamiltonian, which is absent in the SM. A crucial problem in the new physics search within flavour physics in the exclusive decays is the optimal separation of NP effects from uncertainties. It is well known that inclusive decay modes are dominated by partonic contributions; non–perturbative corrections are in general rather smaller[12]. Also, ratios of exclusive decay modes such as asymmetries for $B \to K(\ K^*,\ \rho,\ \gamma)\ \ell^+\ell^-$ decays [13]–[17] are well studied for NP search. Here, large parts of the hadronic uncertainties partially cancel out. The universal extra dimension with only one UED belongs to the classes of NP, where the Wilson coefficients is modified by KK contributions [6, 7] in the penguin and box diagrams. Obviously, these modifications will affect the physical observables. In this connection, we try to investigate the effects of one universal extra dimension on the double–lepton polarization and polarized forward–backward(FB) asymmetries of the $b \to s\ell^+\ell^-$ transition, where the single-lepton polarization asymmetries in the same scenario studied in Ref.[5]. Also, it is well known that the study of the lepton polarization asymmetries are in particular interesting since they are sensitive to the structure of interactions which can be used as a good tool to test not only the SM but also its extensions[13]. Moreover, It is already noted that the study of some of the single lepton polarization asymmetries which are small might not provide sufficient number of observables for checking the structure of the effective Hamiltonian. On the other hand, Considering the polarizations of both leptons, which are supposed to measure simultaneously, we are able to establish the maximum number of independent polarization observables[18].

The plan of the paper is the following: In Section 2 we recall the effective Hamiltonian inducing $b \to s\ell^+\ell^-$ transitions in the SM and in the ACD model, together with the definition of the polarization asymmetries considering in our study. In this Section, we also present the lepton polarization and FB asymmetries for inclusive $b \to s\ell^+\ell^-$ transition. Section 3 includes numerically analyzing the physical observables and conclusions are presented in section 4.

2 Matrix element $b \to s\ell^+\ell^-$ in the ACD model

In the SM, the QCD corrected Hamiltonian for the transitions $b \to s\ell^+\ell^-$ can be achieved by integrating out the heavy quarks and the heavy electroweak bosons[16]:

$$H_W \ = \ 4\,\frac{G_F}{\sqrt{2}} V_{tb} V_{ts}^* \sum_{i=1}^{10} C_i(\mu) O_i(\mu) \tag{1}$$

obtained by a renormalization group evolution from the electroweak scale down to $\mu \simeq m_b$. G_F is the Fermi constant, V_{ij} are elements of the Cabibbo-Kobayashi-Maskawa (CKM) matrix, O_i are the local operators and C_i are Wilson coefficients calculated in naive dimensional regularization (NDR) scheme at the leading order (LO), next-to-leading order

(NLO), and next-to-next-to leading order (NNLO) in the SM[20]–[29].

The effect of the new states predicted in the ACD model comes through the modification of the Wilson coefficients and the operator structures remain the same as SM. In particular, the coefficients acquire a dependence on the compactification radius R. Considering the KK modes effects in the penguin and box diagrams, the above coefficients have been obtained at LO [6, 7]. Clearly, they depend on the additional ACD parameter i.e., R. For large values of $1/R$ the SM values of the Wilson coefficients can be achieved. In general, the coefficients can be expressed in terms of functions $F(x_t, 1/R)$, with $x_t = \dfrac{m_t^2}{M_W^2}$ and m_t is the top quark mass. These functions are generalizations of the corresponding SM functions such as $F_0(x_t)$ according to:

$$F(x_t, 1/R) = F_0(x_t) + \sum_{n=1}^{\infty} F_n(x_t, x_n)\,, \tag{2}$$

with $x_n = \dfrac{m_n^2}{M_W^2}$ and $m_n = \dfrac{n}{R}$. The Glashow-Illiopoulos-Maiani (GIM) mechanism guarantees the finiteness of the Eq. (2) and fulfills the condition $F(x_t, 1/R) \to F_0(x_t)$ when $R \to 0$ [6, 7]. However, as far as $1/R$ is taken in the order of a few hundreds of GeV, the coefficients differ from the SM value: in particular, C_{10} is enhanced and C_7 is suppressed. Obviously, such deviations could be seen in various observables in the inclusive and exclusive B decays.

In the following, we only consider the contribution of the operators O_7, O_9, and O_{10}. Note that we ignore the $O(\alpha_s)$ correction coming from one gluon exchange in the matrix element of the operator $\mathcal{O}_9$ [24], one–loop corrections to the four–quark operators O_1–O_6 which are small [21] and also the long-distance resonance effects. However, a more complimentary and supplementary analysis of the above decay has to be taken into account not only the long-distance contributions, which have their origin in real intermediate $c\bar{c}$ family[23] but also $O(\alpha_s)$ correction. The Wilson coefficients C_7, C_9, and C_{10} in the ACD are real and their explicit expressions can be found in Refs.[6, 7].

In order to compute the polarization asymmetries, one has to choose a reference frame to define the spin directions. A reference frame can be chosen in the center of mass (CM) of the leptons where they move back to back. In such reference frames, if we suppose that ℓ^- moves in the z positive direction and the fact that momentum must conserve, the s and b quarks move in the same direction. In this reference frame, the 4-vector $s^\mu_{\ell^-}$ can be obtained as follows after the Lorentz boost from its rest frame[18]:

$$s^\mu_{\ell^-} = \left\{ \frac{P}{m_\ell} s_z^-, s_x^-, s_y^-, \frac{\sqrt{P^2 + m_\ell^2}}{m_\ell} s_z^- \right\} \quad , \quad s^\mu_{\ell^+} = \left\{ -\frac{P}{m_\ell} s_z^+, s_x^+, s_y^+, \frac{\sqrt{P^2 + m_\ell^2}}{m_\ell} s_z^+ \right\} . \tag{3}$$

The $\hat{s} = \frac{q^2}{m_b^2}$ dependent double–lepton polarization asymmetries $\mathcal{P}_{ij}$ are obtained by evaluating

$$\mathcal{P}_{ij} = \frac{\left[\frac{d\Gamma(\mathbf{s}^+=\hat{\mathbf{i}},\mathbf{s}^-=\hat{\mathbf{j}})}{d\hat{s}} - \frac{d\Gamma(\mathbf{s}^+=\hat{\mathbf{i}},\mathbf{s}^-=-\hat{\mathbf{j}})}{d\hat{s}}\right] - \left[\frac{d\Gamma(\mathbf{s}^+=-\hat{\mathbf{i}},\mathbf{s}^-=\hat{\mathbf{j}})}{d\hat{s}} - \frac{d\Gamma(\mathbf{s}^+=-\hat{\mathbf{i}},\mathbf{s}^-=-\hat{\mathbf{j}})}{d\hat{s}}\right]}{\left[\frac{d\Gamma(\mathbf{s}^+=\hat{\mathbf{i}},\mathbf{s}^-=\hat{\mathbf{j}})}{d\hat{s}} + \frac{d\Gamma(\mathbf{s}^+=\hat{\mathbf{i}},\mathbf{s}^-=-\hat{\mathbf{j}})}{d\hat{s}}\right] + \left[\frac{d\Gamma(\mathbf{s}^+=-\hat{\mathbf{i}},\mathbf{s}^-=\hat{\mathbf{j}})}{d\hat{s}} + \frac{d\Gamma(\mathbf{s}^+=-\hat{\mathbf{i}},\mathbf{s}^-=-\hat{\mathbf{j}})}{d\hat{s}}\right]}, \tag{4}$$

where $\hat{i}$ and $\hat{j}$ are unit vectors[30].

With our choice of reference frame in Eq. (3), the decay happens in two dimensions i.e., the yz plane. In this frame, just the components of the spin can be in the $\hat{x}$ direction. Therefore, any terms including the spin along the $\hat{x}$ direction are as a result of either the dot product of two spins or triple-product correlation with one spin along the $\hat{x}$ direction(i.e., $\mathcal{P}_{xx}$, $\mathcal{P}_{xy}$, and $\mathcal{P}_{xz}$). This holds even in the presence of any extension of the SM. Among these quantities, $\mathcal{P}_{xy}$ and $\mathcal{P}_{xz}$ are attractive which probes the imaginary parts of the products of Wilson coefficients[18]. The expressions for the $\mathcal{P}_{ij}$ asymmetries in $b \to s\ell^+\ell^-$ can be derived from the transition amplitude

$$\begin{aligned}\mathcal{M} = \frac{G_F}{\sqrt{2}} V_{tb}V_{ts}^* \frac{\alpha}{\pi} \quad \Big[& \quad C_9(\mu,1/R)\,\bar{s}_L\gamma_\mu b_L \bar{\ell}\gamma_\mu \ell + C_{10}(\mu,1/R)\,\bar{s}_L\gamma_\mu b_L \bar{\ell}\gamma_\mu\gamma_5\ell \\ & - \quad 2C_7(\mu,1/R)\,\frac{q^\nu}{q^2}\,\left[m_b \bar{s}_L i\sigma_{\mu\nu} b_R + m_s \bar{s}_R i\sigma_{\mu\nu} b_L\right]\bar{\ell}\gamma_\mu\ell\Big]. \end{aligned} \tag{5}$$

Note that the measurements of such asymmetries can give more information about the Wilson coefficients [13].

The $\mathcal{P}_{ij}$ take the form

$$\begin{aligned}
\mathcal{P}_{xx} &= \frac{1}{\Delta}\Bigg\{24Re[C_7(\mu,1/R)C_9^*(\mu,1/R)]\frac{\hat{m}_\ell^2}{\hat{s}} + 4|C_7(\mu,1/R)|^2\frac{(-1+\hat{s})\hat{s}+2(2+\hat{s})\hat{m}_\ell^2}{\hat{s}^2} \\
&\quad +(|C_9(\mu,1/R)|^2 - |C_{10}(\mu,1/R)|^2)\frac{(1-\hat{s})\hat{s}+2(1+2\hat{s})\hat{m}_\ell^2}{\hat{s}}\Bigg\}, && (6)\\
\mathcal{P}_{yx} &= \frac{-2}{\Delta}\, Im[C_9(\mu,1/R)C_{10}^*(\mu,1/R)](1-\hat{s})\sqrt{1-\frac{4\hat{m}_\ell^2}{\hat{s}}}, && (7)\\
\mathcal{P}_{xy} &= \mathcal{P}_{yx}, && (8)\\
\mathcal{P}_{zx} &= \frac{-3\pi}{2\sqrt{\hat{s}}\Delta}\hat{m}_\ell\left\{2Im[C_7(\mu,1/R)C_{10}^*(\mu,1/R)] + Im[C_9(\mu,1/R)C_{10}^*(\mu,1/R)]\right\}, && (9)\\
\mathcal{P}_{yy} &= \frac{1}{\Delta}\Bigg\{24Re[C_7(\mu,1/R)C_9^*(\mu,1/R)]\frac{\hat{m}_\ell^2}{\hat{s}} - 4(|C_9(\mu,1/R)|^2 + |C_{10}(\mu,1/R)|^2)\frac{(1-\hat{s})\hat{m}_\ell^2}{\hat{s}} \\
&\quad +(|C_9(\mu,1/R)|^2 - |C_{10}(\mu,1/R)|^2)((-1+\hat{s}) + \frac{6\hat{m}_\ell^2}{\hat{s}}) \\
&\quad +4|C_7(\mu,1/R)|^2\frac{((1-\hat{s})\hat{s}+2(2+\hat{s})\hat{m}_\ell^2)}{\hat{s}^2}\Bigg\}, && (10)\\
\mathcal{P}_{zy} &= \frac{3\pi}{2\sqrt{\hat{s}}\Delta}\hat{m}_\ell\sqrt{1-\frac{4\hat{m}_\ell^2}{\hat{s}}} && (11)\\
&\quad \left\{2Re[C_7(\mu,1/R)C_{10}^*(\mu,1/R)] - |C_{10}(\mu,1/R)|^2 + Re[C_9(\mu,1/R)C_{10}^*(\mu,1/R)]\hat{s}\right\}, \\
\mathcal{P}_{xz} &= -\mathcal{P}_{zx}, && (12)\\
\mathcal{P}_{yz} &= \frac{3\pi}{2\sqrt{\hat{s}}\Delta}\hat{m}_\ell\sqrt{1-\frac{4\hat{m}_\ell^2}{\hat{s}}} && (13)\\
&\quad \left\{2Re[C_7(\mu,1/R)C_{10}^*(\mu,1/R)] + |C_{10}(\mu,1/R)|^2 + Re[C_9(\mu,1/R)C_{10}^*(\mu,1/R)]\hat{s}\right\},
\end{aligned}$$

$$\begin{aligned}
\mathcal{P}_{zz} &= \frac{1}{2\Delta}\Big\{12Re[C_7(\mu,1/R)C_9^*(\mu,1/R)](1-\frac{2\hat{m}_\ell^2}{\hat{s}})+\frac{4|C_7(\mu,1/R)|^2(2+\hat{s})(1-\frac{2\hat{m}_\ell^2}{\hat{s}})}{\hat{s}} \\
&+(|C_9(\mu,1/R)|^2+|C_{10}(\mu,1/R)|^2)(1+2\hat{s}-\frac{6(1+\hat{s})\hat{m}_\ell^2}{\hat{s}}) \\
&+\frac{2(|C_9(\mu,1/R)|^2-|C_{10}(\mu,1/R)|^2)(2+\hat{s})\hat{m}_\ell^2}{\hat{s}}\Big\}. \qquad (14)
\end{aligned}$$

Except $\mathcal{P}_{zz}$ which is 2 times smaller than the one obtained in Ref. [18], the other $\mathcal{P}_{ij}$'s calculated in Ref. [18] can be achieved by the replacement of $C_i(\mu,1/R) \to C_i^{eff}$ where $i = 7,\ 9,\ 10$. Also, it is obvious that the asymmetries proportional to the imaginary parts of the Wilson coefficients are small in the SM and vanish in the ACD where all Wilson coefficients are considered to be real.

Equipped with the definition of the spin directions of Eq. (3) in the CM frame of leptons, we can evaluate the forward-backward asymmetries corresponding to various polarization components of the ℓ^- and/or ℓ^+ spin by writing[18]:

$$\begin{aligned}
A_{FB}(\mathbf{s}^+,\mathbf{s}^-,\hat{s}) &= A_{FB}(\hat{s})+\Big[\mathcal{A}_x^- s_x^- + \mathcal{A}_y^- s_y^- + \mathcal{A}_z^- s_z^- + \mathcal{A}_x^+ s_x^+ + \mathcal{A}_y^+ s_y^+ + \mathcal{A}_z^+ s_z^+ \\
&+ \mathcal{A}_{xx} s_x^+ s_x^- + \mathcal{A}_{xy} s_x^+ s_y^- + \mathcal{A}_{xz} s_x^+ s_z^- \\
&+ \mathcal{A}_{yx} s_y^+ s_x^- + \mathcal{A}_{yy} s_y^+ s_y^- + \mathcal{A}_{yz} s_y^+ s_z^- \\
&+ \mathcal{A}_{zx} s_z^+ s_x^- + \mathcal{A}_{zy} s_z^+ s_y^- + \mathcal{A}_{zz} s_z^+ s_z^-\Big]\ . \qquad (15)
\end{aligned}$$

The different polarized forward-backward asymmetries are then calculated as follows:

$$\begin{aligned}
\mathcal{A}_x^+ &= 0, \qquad (16)\\
\mathcal{A}_y^+ &= \frac{2}{\Delta}\,\mathrm{Re}(C_9(\mu,1/R)C_{10}^*(\mu,1/R))\,\frac{(1-\hat{s})\,\hat{m}_\ell}{\sqrt{\hat{s}}}\sqrt{1-\frac{4\,\hat{m}_\ell^2}{\hat{s}}}, \qquad (17)\\
\mathcal{A}_z^+ &= \frac{1}{\Delta}\Big\{6\,\mathrm{Re}(C_7(\mu,1/R)C_9^*(\mu,1/R))-\frac{6\,|C_7(\mu,1/R)|^2}{\hat{s}} \\
&-3\,(\,|C_9(\mu,1/R)|^2-|C_{10}(\mu,1/R)|^2)\,\hat{m}_\ell^2 \\
&-12\,\mathrm{Re}(C_7(\mu,1/R)C_{10}^*(\mu,1/R))\,\frac{\hat{m}_\ell^2}{\hat{s}}-\ 6\,\mathrm{Re}(C_9(\mu,1/R)C_{10}^*(\mu,1/R))\,\frac{\hat{m}_\ell^2}{\hat{s}} \\
&-\frac{3}{2}\,(\,|C_9(\mu,1/R)|^2+|C_{10}(\mu,1/R)|^2)\,\hat{s}\,(1-\frac{2\,\hat{m}_\ell^2}{\hat{s}})\Big\}, \qquad (18)\\
\mathcal{A}_x^- &= 0, \qquad (19)\\
\mathcal{A}_y^- &= \mathcal{A}_y^+, \qquad (20)\\
\mathcal{A}_z^- &= \frac{1}{\Delta}\Big\{-6\,\mathrm{Re}(C_7(\mu,1/R)C_9^*(\mu,1/R))-\frac{6\,|C_7(\mu,1/R)|^2}{\hat{s}} \\
&-3\,(\,|C_9(\mu,1/R)|^2-|C_{10}(\mu,1/R)|^2)\,\hat{m}_\ell^2 \\
&+12\,\mathrm{Re}(C_7(\mu,1/R)C_{10}^*(\mu,1/R))\,\frac{\hat{m}_\ell^2}{\hat{s}}+\ 6\,\mathrm{Re}(C_9(\mu,1/R)C_{10}^*(\mu,1/R))\,\frac{\hat{m}_\ell^2}{\hat{s}} \\
&-\frac{3}{2}\,(\,|C_9(\mu,1/R)|^2+|C_{10}(\mu,1/R)|^2)\,\hat{s}\,(1-\frac{2\,\hat{m}_\ell^2}{\hat{s}})\Big\}, \qquad (21)
\end{aligned}$$

$$\mathcal{A}_{xx} = 0, \tag{22}$$

$$\mathcal{A}_{xy} = \frac{-6}{\Delta}\left(2\,\mathrm{Im}(C_7(\mu,1/R)\,C_{10}^*(\mu,1/R)) + \mathrm{Im}(C_9(\mu,1/R)\,C_{10}^*(\mu,1/R))\right)\frac{\hat{m}_\ell^2}{\hat{s}}, \tag{23}$$

$$\mathcal{A}_{xz} = \frac{2}{\Delta}\,\mathrm{Im}(C_9(\mu,1/R)C_{10}^*(\mu,1/R))\,\frac{(1-\hat{s})\,\hat{m}_\ell}{\sqrt{\hat{s}}}\sqrt{1-\frac{4\,\hat{m}_\ell^2}{\hat{s}}}, \tag{24}$$

$$\mathcal{A}_{yx} = -\mathcal{A}_{xy}, \tag{25}$$

$$\mathcal{A}_{yy} = 0, \tag{26}$$

$$\mathcal{A}_{yz} = \left(2|C_9(\mu,1/R)|^2 - \frac{8\,|C_7(\mu,1/R)|^2}{\hat{s}}\right)\frac{(1-\hat{s})\,\hat{m}_\ell}{\Delta\sqrt{\hat{s}}}, \tag{27}$$

$$\mathcal{A}_{zx} = \mathcal{A}_{xz}, \tag{28}$$

$$\mathcal{A}_{zy} = \mathcal{A}_{yz}, \tag{29}$$

$$\mathcal{A}_{zz} = \frac{-3}{\Delta}\left(2\,\mathrm{Re}(C_7(\mu,1/R)\,C_{10}^*(\mu,1/R)) + \mathrm{Re}(C_9(\mu,1/R)\,C_{10}^*(\mu,1/R))\,\hat{s}\right)\sqrt{1-\frac{4\,\hat{m}_\ell^2}{\hat{s}}}\ . \tag{30}$$

Here, $\mathcal{A}_{zz}$ coincides with $-\mathcal{A}_{FB}$ in the SM and any of its extensions[18], provided that the operator structure remains the same. In other words, a significant difference between $\mathcal{A}_{zz}$ and $\mathcal{A}_{FB}$ happens when the new type of interactions are taken into account in the effective Hamiltonian, i.e., the tensor type and scalar type interactions differ between $\mathcal{A}_{zz}$ and $\mathcal{A}_{FB}$[15].

Note that, $\mathcal{A}_{ij}$ coefficients calculated in Ref. [18] can again be obtained by the replacement of $C_i(\mu,1/R) \to C_i^{eff}$ where $i = 7,\ 9,\ 10$.

3 Numerical analysis

In this section, we study the dependence of the double-lepton polarization and the polarized lepton FB asymmetries on the compactification parameters($1/R$). We use the SM parameters shown in Table 1:

Parameter	Value
$\alpha_s(m_Z)$	0.119
α_{em}	1/129
m_W	80.41 (GeV)
m_Z	91.18 (GeV)
$sin^2(\theta_W)$	0.223
m_b	4.7 (GeV)
m_μ	0.106 (GeV)
m_τ	1.780 (GeV)

Table 1: The values of the input parameters used in the numerical calculations.

The allowed range in the ACD model for the Wolfenstein parameters shows a small discrepancy in terms of $1/R$ with respect to the SM values[6].

The physical observables depend on compactification radius (R) and $\hat{s}$. The conservation of KK parity $(-1)^j$, with j as the KK number, implies the absence of tree-level contribution of KK states at the low energy regime. This allows us to establish a bound: $1/R > 250\ GeV$ by the analysis of Tevatron run I data[4]. The same bound can be obtained by the analysis of measured branching ratio of $B \to X_s\gamma$ decay[6, 7]. A sharper constraint on $1/R$ is established by taking into account the leading order contributions due to the exchange of Kaluza-Klein modes as well as the available next-to-next-to-leading order corrections to the branching ratio of $B \to X_s\gamma$ decay [8]. In what follows, we consider $200 < 1/R < 1000\ GeV$. Furthermore, in order to do two-dimensional analysis about the observables, we must eliminate one of the variables either $1/R$ or $\hat{s}$. We do two types of analysis, first, we choose fixed values of the $1/R \sim \{200, 350, 500\}\ GeV$ and look at the $\hat{s}$ dependency of the FB asymmetries. Not that, zero point position of the FB asymmetries in terms of the $\hat{s}$ is less sensitive to the hadronic uncertainties in exclusive decay channels. Second, we eliminate the $\hat{s}$ dependency from double-lepton polarization asymmetries by performing integration over $\hat{s}$ in the allowed region, i.e., we consider the averaged values of the various asymmetries. The average gained over $\hat{s}$ is defined as:

$$\langle \mathcal{P} \rangle = \frac{\int_{4\hat{m}_\ell^2}^{(1-\sqrt{\hat{r}_K})^2} \mathcal{P} \frac{d\mathcal{B}}{d\hat{s}} d\hat{s}}{\int_{4\hat{m}_\ell^2}^{(1-\sqrt{\hat{r}_K})^2} \frac{d\mathcal{B}}{d\hat{s}} d\hat{s}} \ .$$

Our quantitative analysis indicates that some of the observables are less sensitive to the $1/R$; i.e., the maximum deviations from the SM are $\sim 1\%$. We do not present those dependencies on the $1/R$ with relevant figures. We present our analysis for strongly dependent functions in a series of figures. We do not present some of the observables where the SM and ACD values are almost vanishing or their deviation with respect to the SM values are negligible (less than 1%).

From these figures, we deduce the following results:

3.1 Differential polarized FB asymmetries

Figures 1–7 depict the $\hat{s}$ dependency of the single or double-lepton polarization FB asymmetries for three fixed value of the $1/R = 200; 350; 500\ GeV$.

- $\mathcal{A}_y^+(\hat{s})$ for μ channel depicts strong dependency in the nonresonance region where $\hat{s} \sim \{0.0-0.02\}$. The magnitude of $\mathcal{A}_y^+$ is enhanced by decreasing the compactification scale $1/R$ for μ channel (see Fig. 1). For high $\hat{s}$ region, which is also a nonresonance region, the discrepancy almost vanishes.

- $\mathcal{A}_z^-(\hat{s})$ for τ lepton and $\mathcal{A}_z^+(\hat{s})$ for μ lepton are suppressed in the ACD model. In particular, when compactification scale $1/R$ is decreased, the deviation corresponding to the SM values is also decreased (see Figs. 2, 3).

- $\mathcal{A}_z^+(\hat{s})$ for the τ channel depicts almost homogenous discrepancy with respect to the SM values in all kinematically allowed regions. While the SM values are always negative, considering the ACD model, it can get positive values at lower momentum transfer region (see Fig. 4). A measurement of sign of this observable can be used in general to probe the NP effects, in particular, to test the ACD model.

- The zero point position and the magnitude of $\mathcal{A}_{yz}(\hat{s})$ for the μ channel is almost in sensitive to the new parameter of the ACD model, i.e., the compactification scale $1/R$ (see Fig. 5).

- $\mathcal{A}_{yz}(\hat{s})$ for the τ channel shows strong dependency at lower momentum transfer region. The magnitude of $\mathcal{A}_{yz}(\hat{s})$ is enhanced by decreasing the compactification scale $1/R$ (see Fig. 6). For high $\hat{s}$ region, which is also a nonresonance region, the discrepancy almost vanishes.

- The zero point position of $\mathcal{A}_{zz}(\hat{s})$ for the μ channel is shifted to left of the SM point. Also, we find that $\mathcal{A}_{zz}(\hat{s})$ coincides with unpolarized FB asymmetries $\mathcal{A}_{FB}(\hat{s})$[see Fig. 7a], which is given in Ref. [7]. The zero point position of $\mathcal{A}_{zz}(\hat{s})$ ($s_0 = 2C_7/C_9$) is sensitive to the C_7/C_9. We show that s_0 is increasing function of $1/R$. The sizable deviation from the corresponding SM value of s_0 occurs at the small values of $1/R$[see Fig.7b]. This point is especially important for the exclusive decays where the hadronic uncertainty almost vanishes at this point.

3.2 Averaged Double-Lepton Polarization Asymmetries

- Taking into account the ACD model, the magnitudes of all double-lepton polarization asymmetries ($\langle \mathcal{P}_{ij} \rangle$), except $\langle \mathcal{P}_{zz} \rangle$, are enhanced. Moreover, the discrepancy is sizable for smaller values of compactification scale $1/R$ (see Figs. 8–14). On the other hand, the $\langle \mathcal{P}_{zz} \rangle$ is suppressed in the ACD model. Measurements of magnitude and sign of these observables are good tools to search for physics beyond the SM, in particular, to look for the UED.

Finally, some remarks are in order:

First, the quantitative estimations about the accessibility to measure the various physical observables are important issues from the experimental point of view. A required number of $B\bar{B}$ pairs in terms of the branching ratio $\mathcal{B}$ at $n\sigma$ level, the efficiencies of the leptons s_1 and s_2, and various asymmetry functions are given as:

$$N = \frac{n^2}{\mathcal{B} s_1 s_2 \langle \mathcal{A} \rangle^2} \ ,$$

where $\mathcal{A}$ can be an asymmetry.

The efficiencies of detection of the τ–leptons range from 50% to 90% for their various decay modes[31]. Also, the error in τ–lepton polarization is estimated to be about 10%−15% [32]. So, the error in measurement of the τ–lepton asymmetries is approximately 20%−30%, and the error in obtaining the number of events is about 50%. It can be understood that in order to detect the asymmetries in the μ and τ channels at the 3σ level with the asymmetry

of $\mathcal{A} = 1\%$ and efficiency of $\tau \sim 0.5$), the minimum number of required events are $N \sim 10^{10}$ and $N \sim 10^{11}$ for μ and τ leptons, respectively.

On the other hand, the number of $B\bar{B}$ pairs produced at LHC are expected to be about $\sim 10^{12}$. Therefore, a typical asymmetry of ($\mathcal{A} = 1\%$) is detectable at LHC. More about these experimental observables can be found in[18].

Second, we should note that one can reexamine the constraint by studying the branching ratio of pureleptonic B decays and the zero point position of forward–backward asymmetry of $B \to K^* \ell^+ \ell^-$ decay. The former is relatively clean and the latter point is almost free of hadronic uncertainties($\sim 5\%$). After having experimental data on pure leptonic B decay and zero point position of FB, we will obtain the better result for the combination of C_9 and C_{10} from pureleptonic B decay and for the C_7/C_9 from zero point position of FB. In order to fix the Wilson coefficients and the structure of the interaction Hamiltonian, we need to study many other observables. For instance, we introduce some of those observables in the present study, which are polarized FB and lepton polarization asymmetries.

Finally, the important issue is to find the evidence and to distinguish the UED model from the others. Even though there are few studies trying to shed light and introduce a way to distinguish the UED from the other models (see for example [33]), this issue is the common problem of all models and nobody has yet found a clear solution.

4 Conclusion

To sum up, we presented the various asymmetries in inclusive $b \to s\ell^+\ell^-$ transition in the ACD model. The result we obtained are:

- The zero point position of double–lepton polarization FB asymmetry in the ACD model is shifted to the left of the SM position.

- Some of the double–lepton polarization and polarized double or single-lepton polarization forward–backward which are already accessible at LHC, depict the strong dependency ($\hat{s}$) on the free parameter of the ACD model, which is compactification scale R.

  Thus, the measurement of zero point position of polarized FB asymmetry as well as sign or magnitude polarized FB and double-lepton polarization asymmetries can serve as a good test for the predictions of the ACD.

5 Acknowledgment

The authors would like to thank T. M. Aliev and A. Ozpineci for their useful discussions. V. Bashiry thanks the Ministry of Education of Turkish Republic of Northern Cyprus for their partially support. Also, M. B. and K. A. would like to thank TUBITAK, Turkish Scientific and Research Council, for their financial support provided under the Project No.103T666.

References

[1] N. Arkani-Hamed, S. Dimopoulos and G. Dvali, Phys. Lett. **B 429**, 263 (1998); Phys. Rev. **D 59**, 086004 (1999); I. Antoniadis, N. Arkani-Hamed, S. Dimopoulos and G. Dvali, Phys. Lett. **B 439**, 257 (1998).

[2] C. Macesanu, C.D. McMullen, S. Nandi, arXiv:hep-ph/0201300.

[3] I. Antoniadis, Phys. Lett. **B 246** 377 (1990).

[4] T. Appelquist, H. C. Cheng and B. A. Dobrescu, Phys. Rev. **D 64**, 035002 (2001).

[5] P. Colangelo, F. De Fazio, R. Ferrandes and T. N. Pham, Phys. Rev. **D 74**, 115006 (2006) [arXiv:hep-ph/0610044].

[6] A.J. Buras, M. Spranger and A. Weiler, Nucl. Phys. **B 660** (2003) 225.

[7] A.J. Buras, A. Poschenrieder, M. Spranger and A. Weiler, Nucl. Phys. **B 678** (2004) 455.

[8] U. Haisch and A. Weiler, Phys. Rev. **D 76**, 034014 (2007).

[9] R. Mohanata and A.K. Giri, Phys. Rev. **D 75**, 035008, (2007).

[10] T.M. Aliev and M. Savci, Eur. Phys. J. **C 50**, 91,(2007).

[11] Ishtiaq Ahmed, M. Ali Paracha and M. Jamil Aslam, arXiv:0802.0740.

[12] T. Hurth, Rev. Mod. Phys. **75** (2003) 1159.

[13] J. L. Hewett, Phys. Rev. **D 53** (1996) 4964.

[14] T. M. Aliev, V. Bashiry and M. Savci, Eur. Phys. J. **C 35** (2004) 197.

[15] T. M. Aliev, V. Bashiry and M. Savci, JHEP **0405** (2004) 037 [arXiv:hep-ph/0403282].

[16] A. Ali, Patricia Ball, L.T. Handoko and G. Hiller, Phys.Rev. **D 61**,074024 (2000).

[17] F. Krüger and L. M. Sehgal *Phys. Lett.* **B 380** (1996) 199.

[18] W. Bensalem, D. London, N. Sinha and R. Sinha, Phys. Rev. **D 67** (2003) 034007.

[19] T. Inami and C. S. Lim, Prog. Theor. Phys. **65**, 297 (1981) [Erratum-ibid. **65**, 1772 (1981)].

[20] A. J. Buras and M. Münz, *Phys. Rev.* **D 52** (1995) 186.

[21] B. Grinstein, M. J. Savage and M. B. Wise, *Nucl. Phys.* **B 319** (1989) 271.

[22] W. S. Hou, R. S. Willey and A. Soni, *Phys. Rev. Lett* **58** (1987) 1608; *ibid* **60** (1988) 2337 *Erratum.*

[23] N. G. Deshpande and J. Trampetic, *Phys. Rev. Lett* **60** (1988) 2583.

[24] M. Jezabek and J. H. Kühn, *Nucl. Phys.* **B 320** (1989) 20.

[25] M. Misiak, Nucl. Phys. **B 393** (1993) 23.

[26] M. Misiak, Nucl. Phys. **B 439** 461(E) (1995).

[27] C. Bobeth, M. Misiak and J. Urban, Nucl. Phys. B **574**, 291 (2000).

[28] P. Gambino, M. Gorbahn and U. Haisch, Nucl. Phys. B **673**, 238 (2003).

[29] T. Huber, E. Lunghi, M. Misiak and D. Wyler, Nucl. Phys. **B 740** (2006) 105.

[30] S. Fukae and C.S. Kim, T. Yoshikawa, Phys. Rev. D **61** (2000) 074015.

[31] G. Abbiendi *et. al*, OPAL Collaboration, Phys. Lett. **B 492**, 23 (2000).

[32] A. Rouge, Workshop on τ lepton physics, Orsay, France (1990).

[33] A. Kundu, arXiv:0806.3815.

Figure captions

Fig. (1) The dependence of the $\mathcal{A}_y^+(\hat{s})$ of $b \to s\mu^+\mu^-$ on $\hat{s}$ for $1/R = 200; 350; 500\ GeV$.

Fig. (2) The dependence of the $\mathcal{A}_z^-(\hat{s})$ of $b \to s\tau^+\tau^-$ on $\hat{s}$ for $1/R = 200; 350; 500\ GeV$.

Fig. (3) The same as in Fig. (1), but for the $\mathcal{A}_z^+(\hat{s})$.

Fig. (4) The same as in Fig. (3), but for the τ lepton.

Fig. (5) The dependence of the $\mathcal{A}_{yz}(\hat{s})$ of $b \to s\mu^+\mu^-$ on $\hat{s}$ for $1/R = 200; 350; 500\ GeV$.

Fig. (6) The same as in Fig. (5), but for the τ lepton.

Fig. (7a) The dependence of the $\mathcal{A}_{zz}(\hat{s})$ of $b \to s\mu^+\mu^-$ on $\hat{s}$ for $1/R = 200; 350; 500\ GeV$.

Fig. (7b) The dependence of the s_0 of $b \to s\mu^+\mu^-$ on $1/R$.

Fig. (8) The dependence of the $\langle \mathcal{P}_{xx} \rangle$ of $b \to s\mu^+\mu^-$ on $1/R$.

Fig. (9) The same as in Fig. (8), but for the τ lepton.

Fig. (10) The dependence of the $\langle \mathcal{P}_{yy} \rangle$ of $b \to s\mu^+\mu^-$ on $1/R$.

Fig. (11) The same as in Fig. (10), but for the τ lepton.

Fig. (12) The dependence of the $\langle \mathcal{P}_{yz} \rangle$ of $b \to s\tau^+\tau^-$ on $1/R$.

Fig. (13) The dependence of the $\langle \mathcal{P}_{zy} \rangle$ of $b \to s\tau^+\tau^-$ on $1/R$.

Fig. (14) The dependence of the $\langle \mathcal{P}_{zz} \rangle$ of $b \to s\tau^+\tau^-$ on $1/R$.

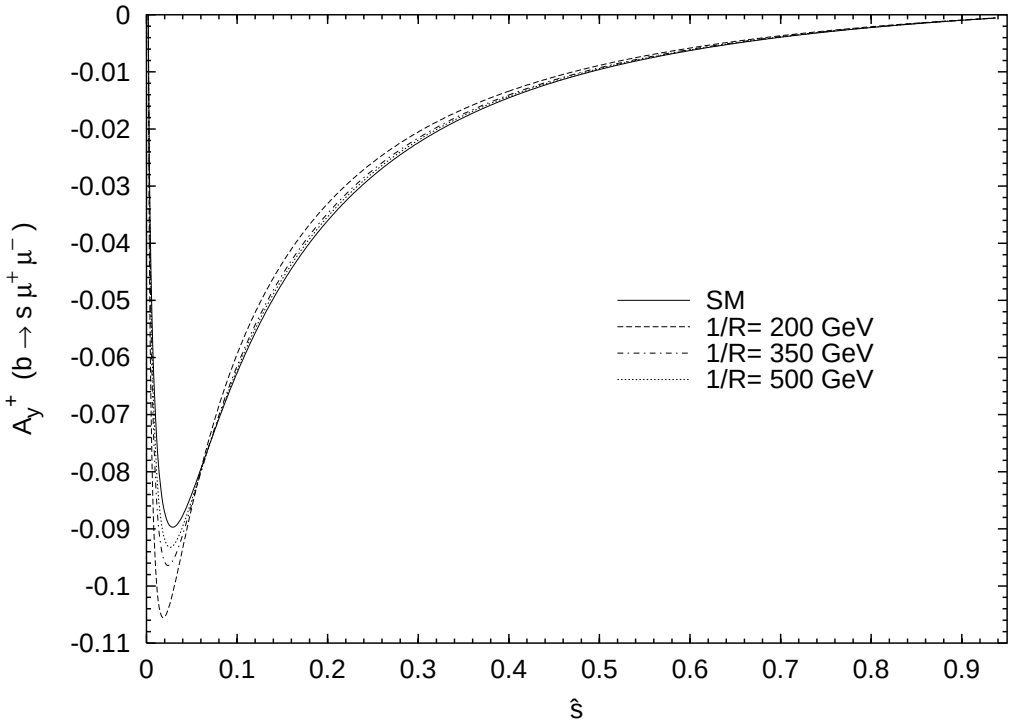

Figure 1:

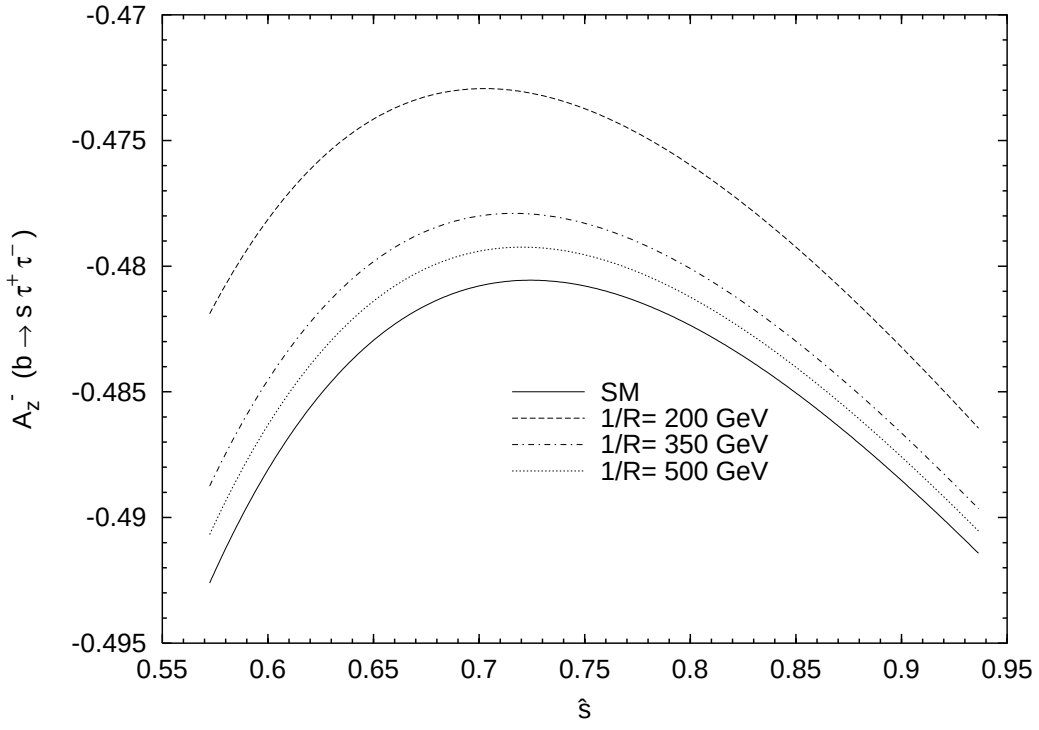

Figure 2:

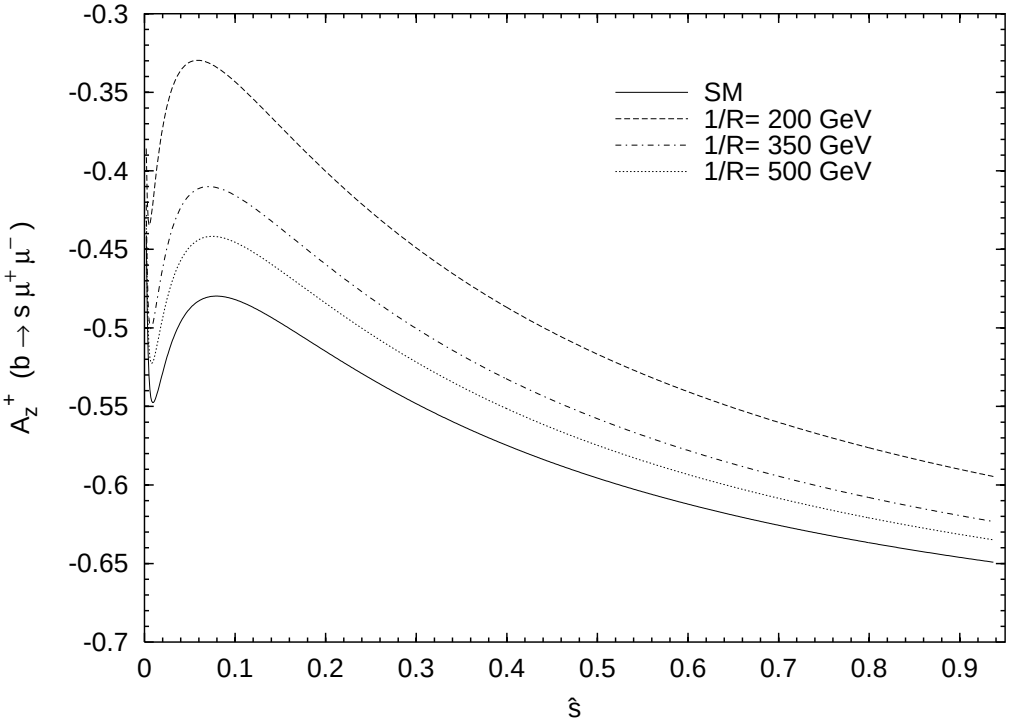

Figure 3:

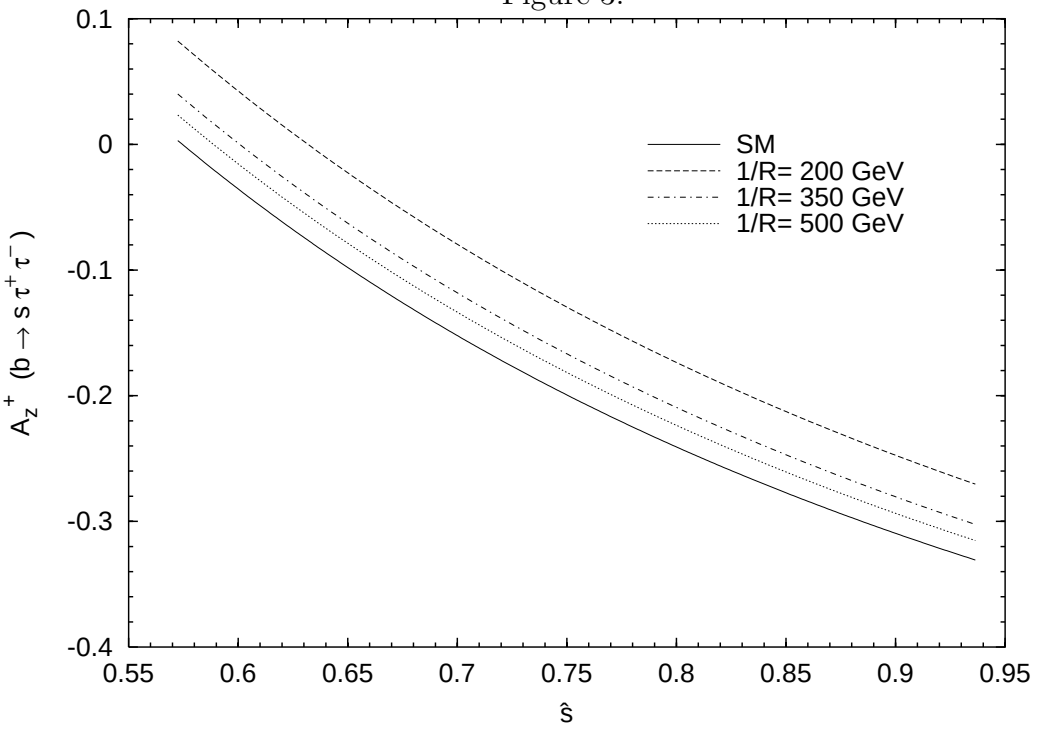

Figure 4:

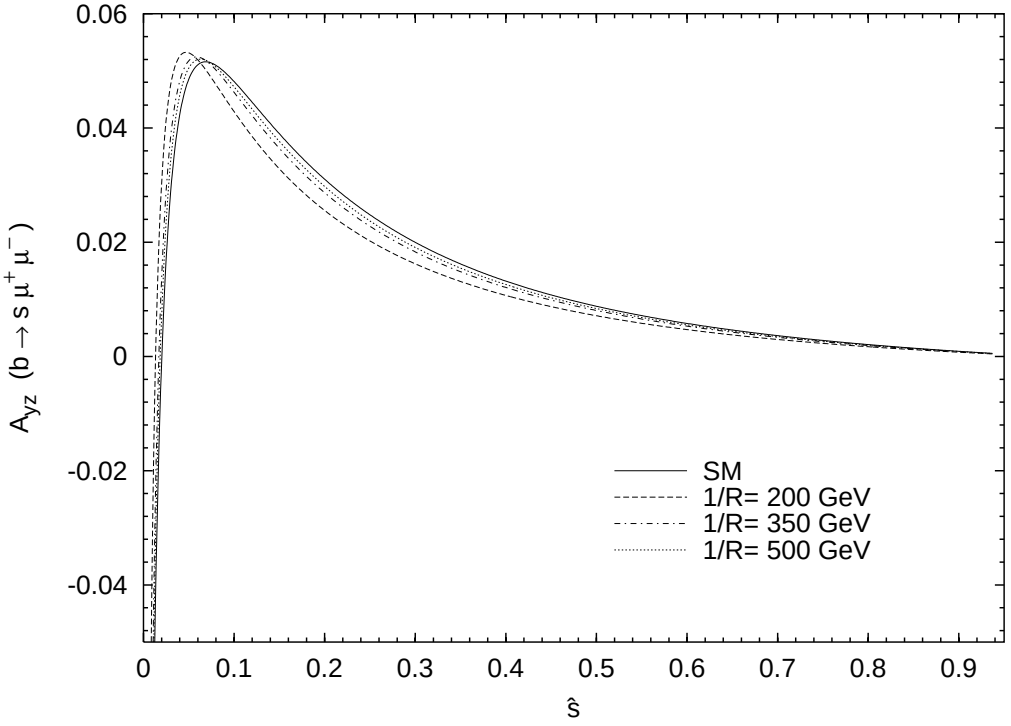

Figure 5:

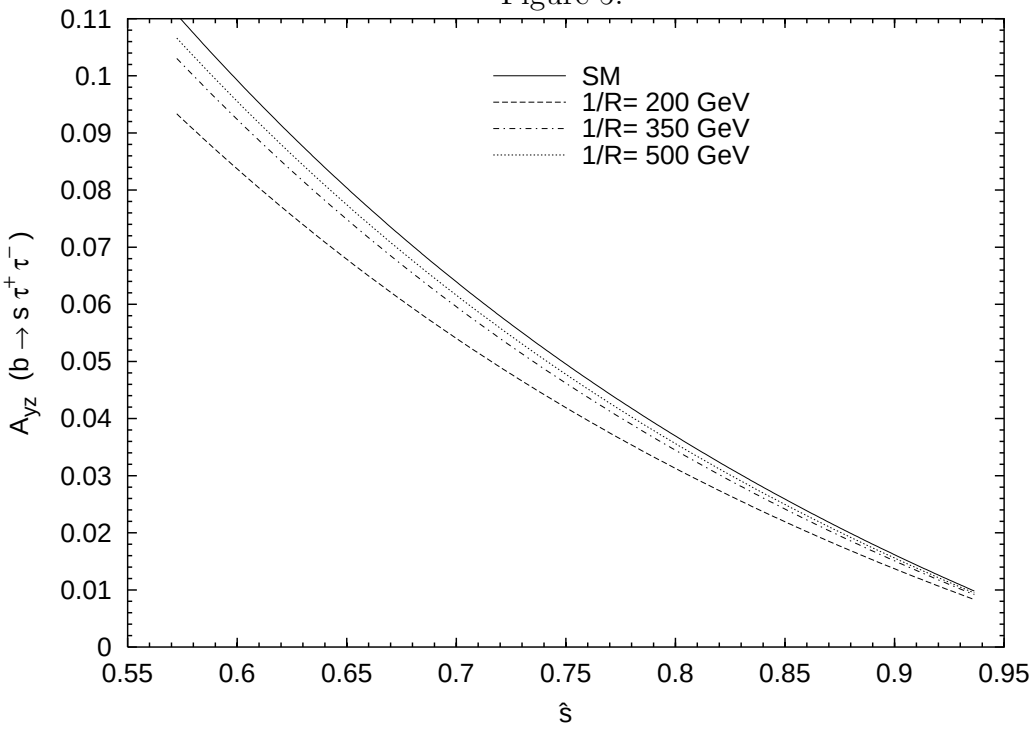

Figure 6:

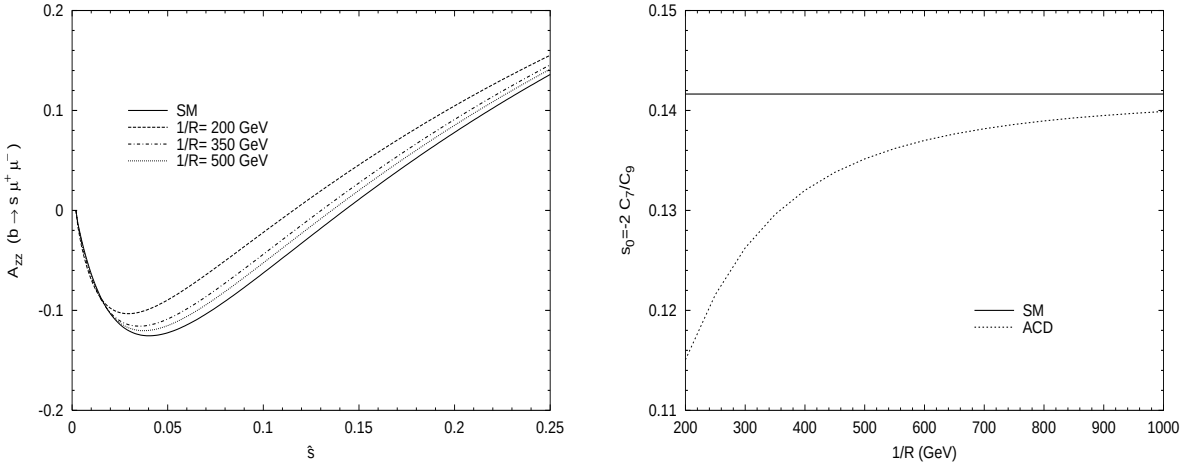

(a) (b)

Figure 7:

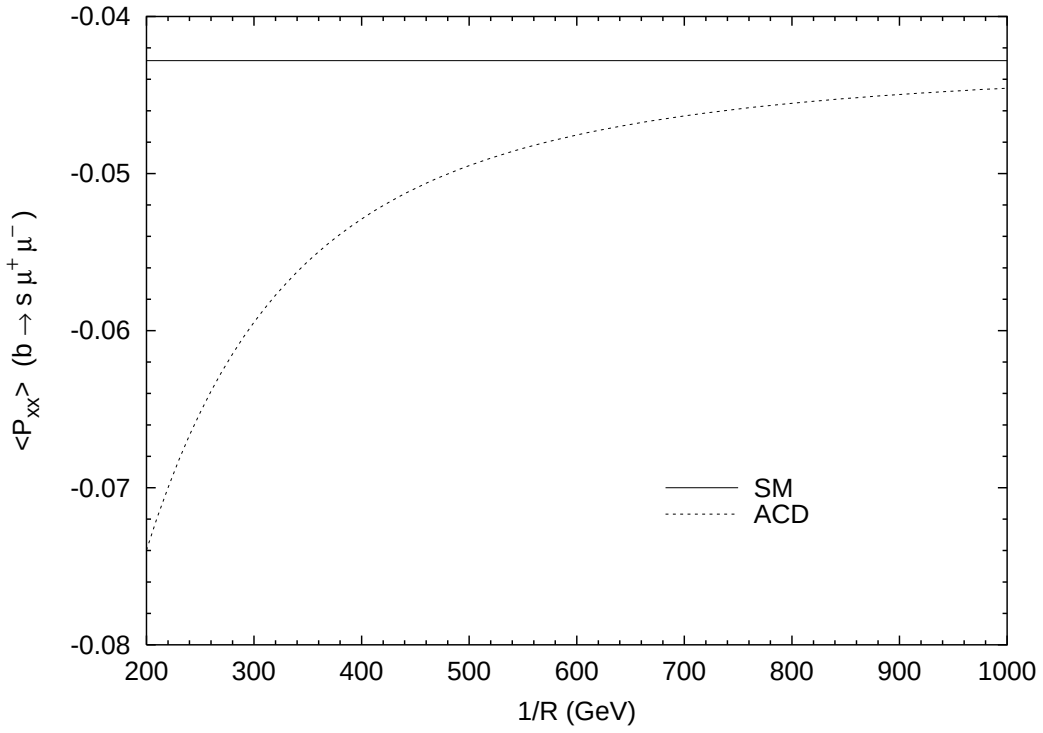

Figure 8:

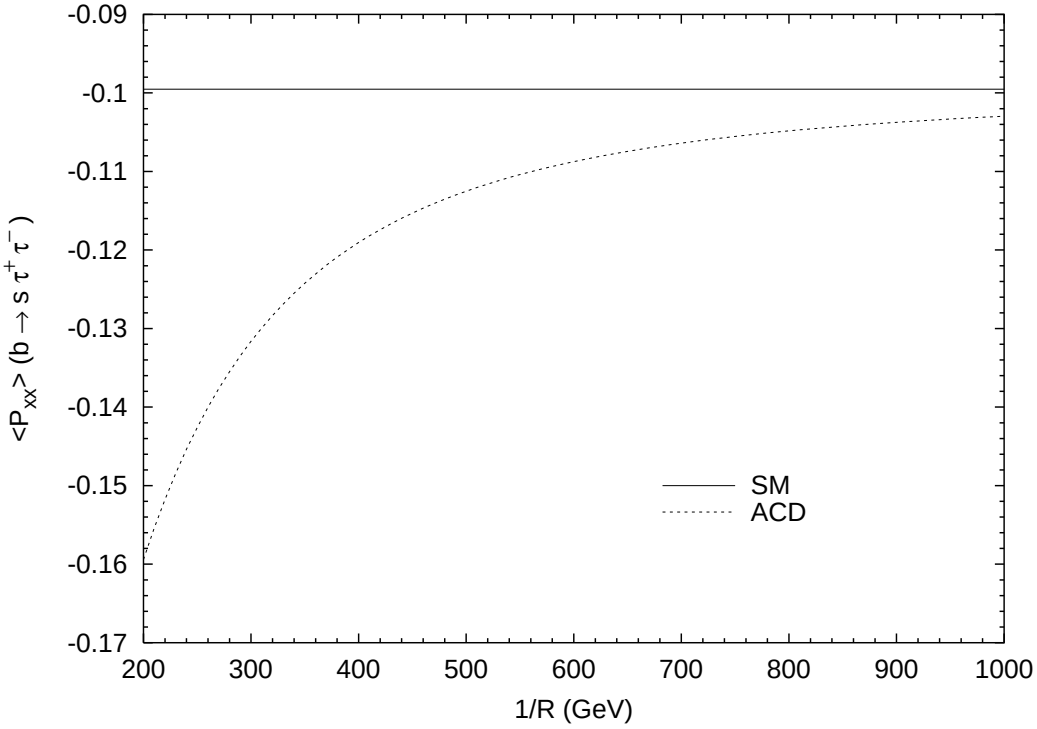

Figure 9:

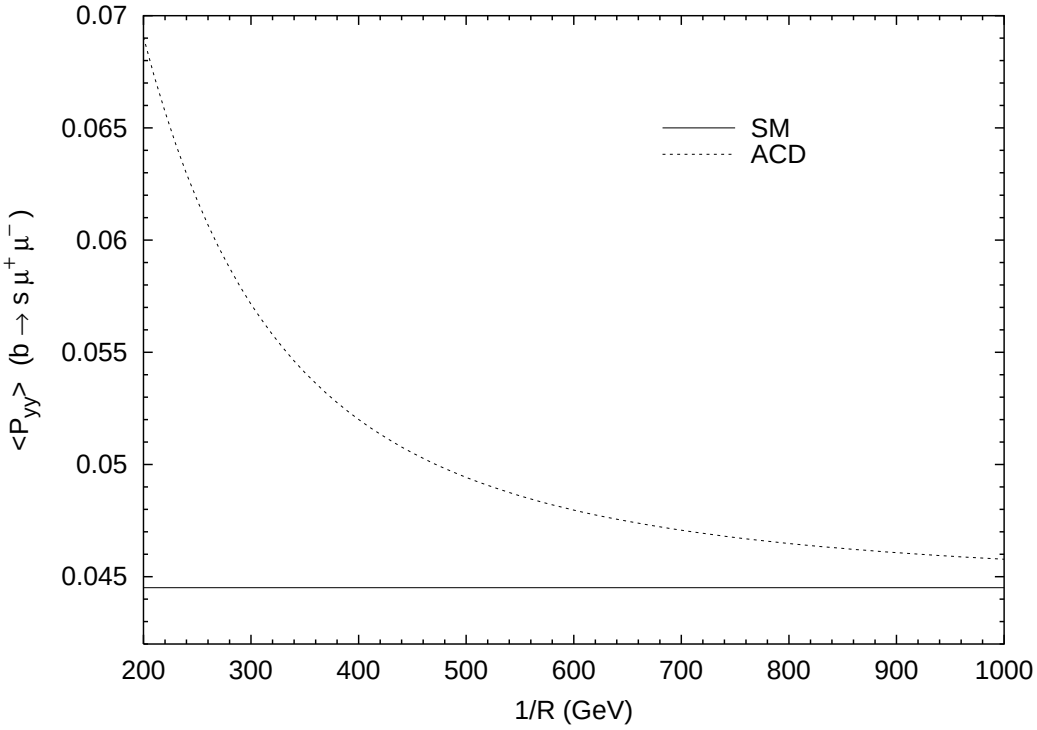

Figure 10:

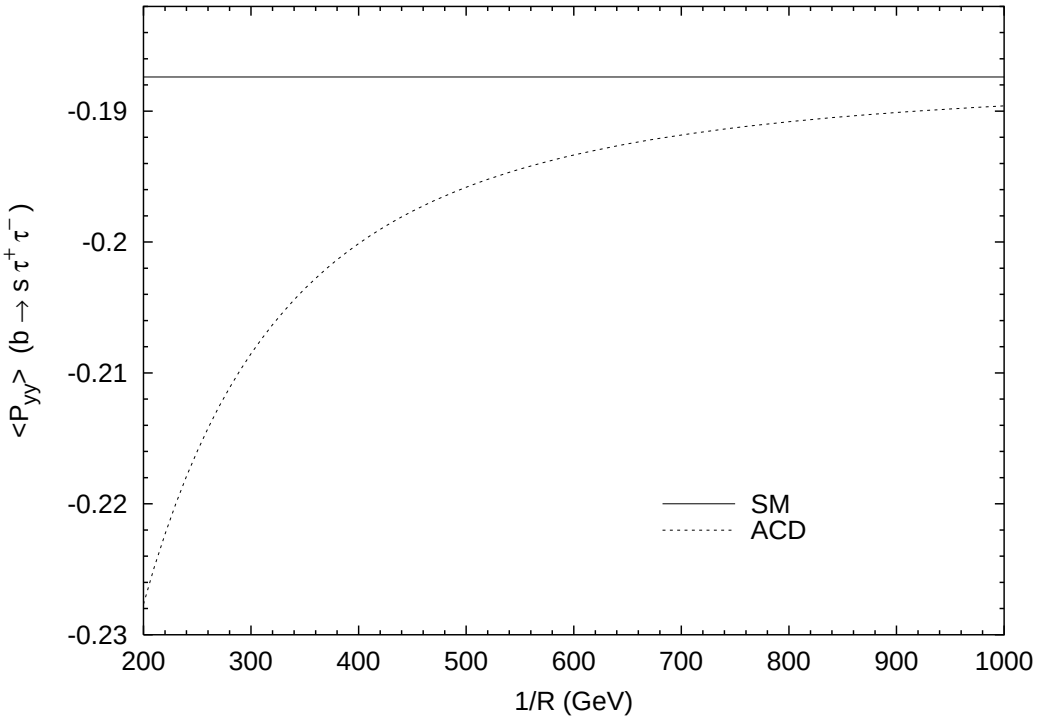

Figure 11:

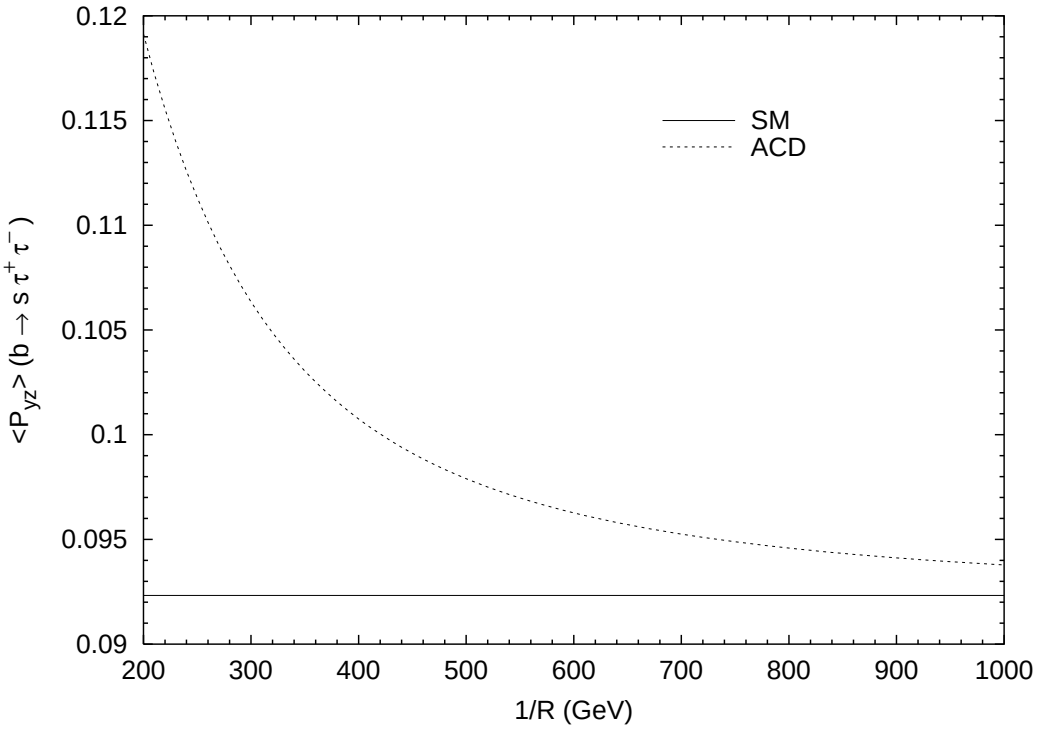

Figure 12:

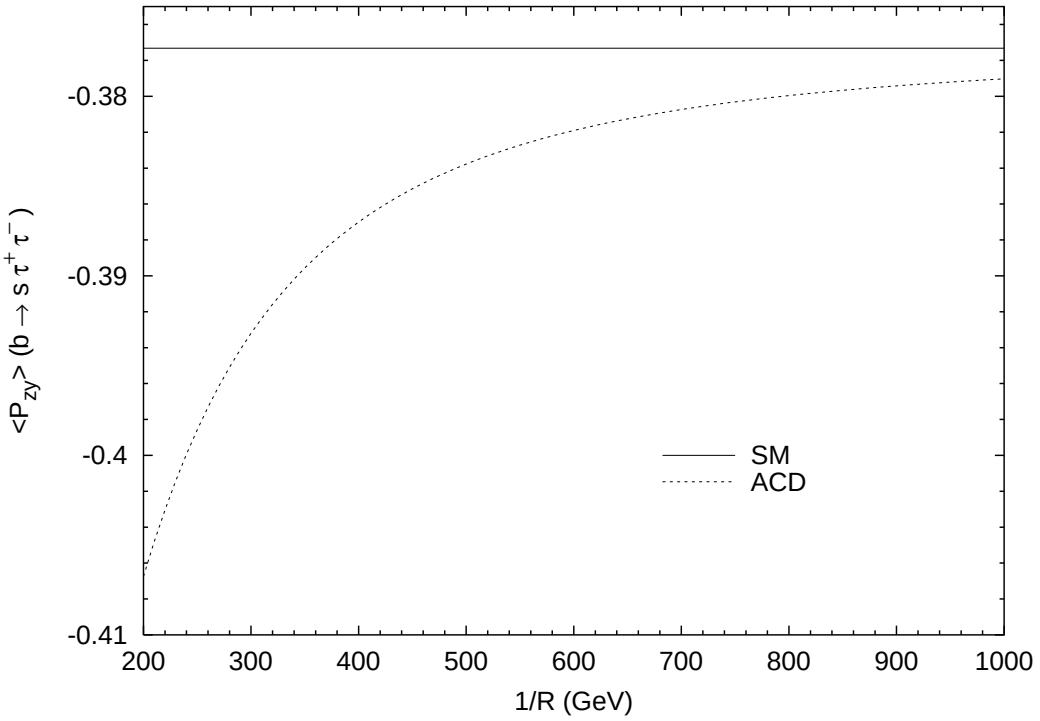

Figure 13:

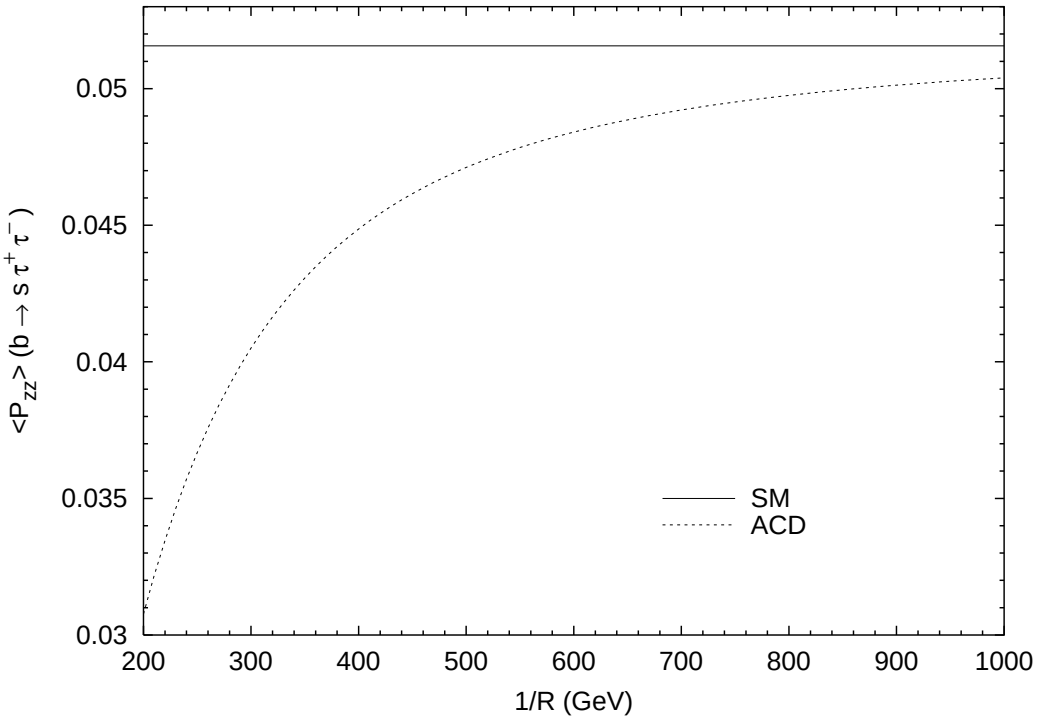

Figure 14: